



First observation of the decay

$$B^+ \rightarrow \pi^+ \mu^+ \mu^-$$

The LHCb collaboration[†]

Abstract

A discovery of the rare decay $B^+ \rightarrow \pi^+ \mu^+ \mu^-$ is presented. This decay is observed for the first time, with 5.2σ significance. The observation is made using pp collision data, corresponding to an integrated luminosity of 1.0 fb^{-1} , collected with the LHCb detector. The measured branching fraction is $(2.3 \pm 0.6 \text{ (stat.)} \pm 0.1 \text{ (syst.)}) \times 10^{-8}$, and the ratio of the $B^+ \rightarrow \pi^+ \mu^+ \mu^-$ and $B^+ \rightarrow K^+ \mu^+ \mu^-$ branching fractions is measured to be $0.053 \pm 0.014 \text{ (stat.)} \pm 0.001 \text{ (syst.)}$.

Published in the Journal of High Energy Physics

[†]Authors are listed on the following pages.

LHCb collaboration

R. Aaij³⁸, C. Abellan Beteta^{33,n}, A. Adametz¹¹, B. Adeva³⁴, M. Adinolfi⁴³, C. Adrover⁶, A. Affolder⁴⁹, Z. Ajaltouni⁵, J. Albrecht³⁵, F. Alessio³⁵, M. Alexander⁴⁸, S. Ali³⁸, G. Alkhazov²⁷, P. Alvarez Cartelle³⁴, A.A. Alves Jr²², S. Amato², Y. Amhis³⁶, L. Anderlini^{17,f}, J. Anderson³⁷, R.B. Appleby⁵¹, O. Aquines Gutierrez¹⁰, F. Archilli^{18,35}, A. Artamonov³², M. Artuso⁵³, E. Aslanides⁶, G. Auriemma^{22,m}, S. Bachmann¹¹, J.J. Back⁴⁵, C. Baesso⁵⁴, V. Balagura²⁸, W. Baldini¹⁶, R.J. Barlow⁵¹, C. Barschel³⁵, S. Barsuk⁷, W. Barter⁴⁴, A. Bates⁴⁸, C. Bauer¹⁰, Th. Bauer³⁸, A. Bay³⁶, J. Beddow⁴⁸, I. Bediaga¹, S. Belogurov²⁸, K. Belous³², I. Belyaev²⁸, E. Ben-Haim⁸, M. Benayoun⁸, G. Bencivenni¹⁸, S. Benson⁴⁷, J. Benton⁴³, A. Berezchnoy²⁹, R. Bernet³⁷, M.-O. Bettler⁴⁴, M. van Beuzekom³⁸, A. Bien¹¹, S. Bifani¹², T. Bird⁵¹, A. Bizzeti^{17,h}, P.M. Bjørnstad⁵¹, T. Blake³⁵, F. Blanc³⁶, C. Blanks⁵⁰, J. Blouw¹¹, S. Blusk⁵³, A. Bobrov³¹, V. Bocci²², A. Bondar³¹, N. Bondar²⁷, W. Bonivento¹⁵, S. Borghi^{48,51}, A. Borgia⁵³, T.J.V. Bowcock⁴⁹, C. Bozzi¹⁶, T. Brambach⁹, J. van den Brand³⁹, J. Bressieux³⁶, D. Brett⁵¹, M. Britsch¹⁰, T. Britton⁵³, N.H. Brook⁴³, H. Brown⁴⁹, A. Büchler-Germann³⁷, I. Burducea²⁶, A. Bursche³⁷, J. Buytaert³⁵, S. Cadeddu¹⁵, O. Callot⁷, M. Calvi^{20,j}, M. Calvo Gomez^{33,n}, A. Camboni³³, P. Campana^{18,35}, A. Carbone^{14,c}, G. Carboni^{21,k}, R. Cardinale^{19,i,35}, A. Cardini¹⁵, L. Carson⁵⁰, K. Carvalho Akiba², G. Casse⁴⁹, M. Cattaneo³⁵, Ch. Cauet⁹, M. Charles⁵², Ph. Charpentier³⁵, P. Chen^{3,36}, N. Chiapolini³⁷, M. Chrzaszcz²³, K. Ciba³⁵, X. Cid Vidal³⁴, G. Ciezarek⁵⁰, P.E.L. Clarke⁴⁷, M. Clemencic³⁵, H.V. Cliff⁴⁴, J. Closier³⁵, C. Coca²⁶, V. Coco³⁸, J. Cogan⁶, E. Cogneras⁵, P. Collins³⁵, A. Comerma-Montells³³, A. Contu⁵², A. Cook⁴³, M. Coombes⁴³, G. Corti³⁵, B. Couturier³⁵, G.A. Cowan³⁶, D. Craik⁴⁵, S. Cunliffe⁵⁰, R. Currie⁴⁷, C. D'Ambrosio³⁵, P. David⁸, P.N.Y. David³⁸, I. De Bonis⁴, K. De Bruyn³⁸, S. De Capua^{21,k}, M. De Cian³⁷, J.M. De Miranda¹, L. De Paula², P. De Simone¹⁸, D. Decamp⁴, M. Deckenhoff⁹, H. Degaudenzi^{36,35}, L. Del Buono⁸, C. Deplano¹⁵, D. Derkach^{14,35}, O. Deschamps⁵, F. Dettori³⁹, J. Dickens⁴⁴, H. Dijkstra³⁵, P. Diniz Batista¹, F. Domingo Bonal^{33,n}, S. Donleavy⁴⁹, F. Dordei¹¹, A. Dosil Suárez³⁴, D. Dossett⁴⁵, A. Dovbnya⁴⁰, F. Dupertuis³⁶, R. Dzhelyadin³², A. Dziurda²³, A. Dzyuba²⁷, S. Easo⁴⁶, U. Egede⁵⁰, V. Egorychev²⁸, S. Eidelman³¹, D. van Eijk³⁸, F. Eisele¹¹, S. Eisenhardt⁴⁷, R. Ekelhof⁹, L. Eklund⁴⁸, I. El Rifai⁵, Ch. Elsasser³⁷, D. Elsby⁴², D. Esperante Pereira³⁴, A. Falabella^{14,e}, C. Färber¹¹, G. Fardell⁴⁷, C. Farinelli³⁸, S. Farry¹², V. Fave³⁶, V. Fernandez Albor³⁴, F. Ferreira Rodrigues¹, M. Ferro-Luzzi³⁵, S. Filippov³⁰, C. Fitzpatrick⁴⁷, M. Fontana¹⁰, F. Fontanelli^{19,i}, R. Forty³⁵, O. Francisco², M. Frank³⁵, C. Frei³⁵, M. Frosini^{17,f}, S. Furcas²⁰, A. Gallas Torreira³⁴, D. Galli^{14,c}, M. Gandelman², P. Gandini⁵², Y. Gao³, J.-C. Garnier³⁵, J. Garofoli⁵³, J. Garra Tico⁴⁴, L. Garrido³³, D. Gascon³³, C. Gaspar³⁵, R. Gauld⁵², E. Gersabeck¹¹, M. Gersabeck³⁵, T. Gershon^{45,35}, Ph. Ghez⁴, V. Gibson⁴⁴, V.V. Gligorov³⁵, C. Göbel⁵⁴, D. Golubkov²⁸, A. Golutvin^{50,28,35}, A. Gomes², H. Gordon⁵², M. Grabalosa Gándara³³, R. Graciani Diaz³³, L.A. Granado Cardoso³⁵, E. Graugés³³, G. Graziani¹⁷, A. Grecu²⁶, E. Greening⁵², S. Gregson⁴⁴, O. Grünberg⁵⁵, B. Gui⁵³, E. Gushchin³⁰, Yu. Guz³², T. Gys³⁵, C. Hadjivasiliou⁵³, G. Haefeli³⁶, C. Haen³⁵, S.C. Haines⁴⁴, S. Hall⁵⁰, T. Hampson⁴³, S. Hansmann-Menzemer¹¹, N. Harnew⁵², S.T. Harnew⁴³, J. Harrison⁵¹, P.F. Harrison⁴⁵, T. Hartmann⁵⁵, J. He⁷, V. Heijne³⁸, K. Hennessy⁴⁹, P. Henrard⁵, J.A. Hernando Morata³⁴, E. van Herwijnen³⁵, E. Hicks⁴⁹, D. Hill⁵², M. Hoballah⁵, P. Hopchev⁴, W. Hulsbergen³⁸, P. Hunt⁵², T. Huse⁴⁹, N. Hussain⁵², R.S. Huston¹², D. Hutchcroft⁴⁹, D. Hynds⁴⁸, V. Iakovenko⁴¹, P. Ilten¹², J. Imong⁴³, R. Jacobsson³⁵, A. Jaeger¹¹, M. Jahjah Hussein⁵, E. Jans³⁸, F. Jansen³⁸, P. Jatton³⁶, B. Jean-Marie⁷, F. Jing³, M. John⁵²,

D. Johnson⁵², C.R. Jones⁴⁴, B. Jost³⁵, M. Kabbalo⁹, S. Kandybei⁴⁰, M. Karacson³⁵,
 T.M. Karbach⁹, J. Keaveney¹², I.R. Kenyon⁴², U. Kerzel³⁵, T. Ketel³⁹, A. Keune³⁶, B. Khanji²⁰,
 Y.M. Kim⁴⁷, M. Knecht³⁶, O. Kochebina⁷, I. Komarov²⁹, R.F. Koopman³⁹, P. Koppenburg³⁸,
 M. Korolev²⁹, A. Kozlinskiy³⁸, L. Kravchuk³⁰, K. Kreplin¹¹, M. Kreps⁴⁵, G. Krocker¹¹,
 P. Krokovny³¹, F. Kruse⁹, M. Kucharczyk^{20,23,35,j}, V. Kudryavtsev³¹, T. Kvaratskheliya^{28,35},
 V.N. La Thi³⁶, D. Lacarrere³⁵, G. Lafferty⁵¹, A. Lai¹⁵, D. Lambert⁴⁷, R.W. Lambert³⁹,
 E. Lanciotti³⁵, G. Lanfranchi^{18,35}, C. Langenbruch³⁵, T. Latham⁴⁵, C. Lazzeroni⁴², R. Le Gac⁶,
 J. van Leerdam³⁸, J.-P. Lees⁴, R. Lefèvre⁵, A. Leflat^{29,35}, J. Lefrançois⁷, O. Leroy⁶, T. Lesiak²³,
 L. Li³, Y. Li³, L. Li Gioi⁵, M. Lieng⁹, M. Liles⁴⁹, R. Lindner³⁵, C. Linn¹¹, B. Liu³, G. Liu³⁵,
 J. von Loeben²⁰, J.H. Lopes², E. Lopez Asamar³³, N. Lopez-March³⁶, H. Lu³, J. Luisier³⁶,
 A. Mac Raighne⁴⁸, F. Machefert⁷, I.V. Machikhiliyan^{4,28}, F. Maciuc¹⁰, O. Maev^{27,35}, J. Magnin¹,
 S. Malde⁵², R.M.D. Mamunur³⁵, G. Manca^{15,d}, G. Mancinelli⁶, N. Mangiafave⁴⁴, U. Marconi¹⁴,
 R. Märki³⁶, J. Marks¹¹, G. Martellotti²², A. Martens⁸, L. Martin⁵², A. Martín Sánchez⁷,
 M. Martinelli³⁸, D. Martinez Santos³⁵, A. Massafferri¹, Z. Mathe¹², C. Matteuzzi²⁰,
 M. Matveev²⁷, E. Maurice⁶, A. Mazurov^{16,30,35}, J. McCarthy⁴², G. McGregor⁵¹, R. McNulty¹²,
 M. Meissner¹¹, M. Merk³⁸, J. Merkel⁹, D.A. Milanese¹³, M.-N. Minard⁴, J. Molina Rodriguez⁵⁴,
 S. Monteil⁵, D. Moran⁵¹, P. Morawski²³, R. Mountain⁵³, I. Mous³⁸, F. Muheim⁴⁷, K. Müller³⁷,
 R. Muresan²⁶, B. Muryn²⁴, B. Muster³⁶, J. Mylroie-Smith⁴⁹, P. Naik⁴³, T. Nakada³⁶,
 R. Nandakumar⁴⁶, I. Nasteva¹, M. Needham⁴⁷, N. Neufeld³⁵, A.D. Nguyen³⁶,
 C. Nguyen-Mau^{36,o}, M. Nicol⁷, V. Niess⁵, N. Nikitin²⁹, T. Nikodem¹¹, A. Nomerotski^{52,35},
 A. Novoselov³², A. Oblakowska-Mucha²⁴, V. Obraztsov³², S. Oggero³⁸, S. Ogilvy⁴⁸,
 O. Okhrimenko⁴¹, R. Oldeman^{15,d,35}, M. Orlandea²⁶, J.M. Otalora Goicochea², P. Owen⁵⁰,
 B.K. Pal⁵³, A. Palano^{13,b}, M. Palutan¹⁸, J. Panman³⁵, A. Papanestis⁴⁶, M. Pappagallo⁴⁸,
 C. Parkes⁵¹, C.J. Parkinson⁵⁰, G. Passaleva¹⁷, G.D. Patel⁴⁹, M. Patel⁵⁰, G.N. Patrick⁴⁶,
 C. Patrignani^{19,i}, C. Pavel-Nicorescu²⁶, A. Pazos Alvarez³⁴, A. Pellegrino³⁸, G. Penso^{22,l},
 M. Pepe Altarelli³⁵, S. Perazzini^{14,c}, D.L. Perego^{20,j}, E. Perez Trigo³⁴,
 A. Pérez-Calero Yzquierdo³³, P. Perret⁵, M. Perrin-Terrin⁶, G. Pessina²⁰, A. Petrolini^{19,i},
 A. Phan⁵³, E. Picatoste Olloqui³³, B. Pie Valls³³, B. Pietrzyk⁴, T. Pilař⁴⁵, D. Pinci²²,
 S. Playfer⁴⁷, M. Plo Casasus³⁴, F. Polci⁸, G. Polok²³, A. Poluektov^{45,31}, E. Polcarpo²,
 D. Popov¹⁰, B. Popovici²⁶, C. Potterat³³, A. Powell⁵², J. Prisciandaro³⁶, V. Pugatch⁴¹,
 A. Puig Navarro³³, W. Qian³, J.H. Rademacker⁴³, B. Rakotomiamanana³⁶, M.S. Rangel²,
 I. Raniuk⁴⁰, N. Rauschmayr³⁵, G. Raven³⁹, S. Redford⁵², M.M. Reid⁴⁵, A.C. dos Reis¹,
 S. Ricciardi⁴⁶, A. Richards⁵⁰, K. Rinnert⁴⁹, D.A. Roa Romero⁵, P. Robbe⁷, E. Rodrigues^{48,51},
 P. Rodriguez Perez³⁴, G.J. Rogers⁴⁴, S. Roiser³⁵, V. Romanovsky³², A. Romero Vidal³⁴,
 M. Rosello^{33,n}, J. Rouvinet³⁶, T. Ruf³⁵, H. Ruiz³³, G. Sabatino^{21,k}, J.J. Saborido Silva³⁴,
 N. Sagidova²⁷, P. Sail⁴⁸, B. Saitta^{15,d}, C. Salzmann³⁷, B. Sanmartin Sedes³⁴, M. Sannino^{19,i},
 R. Santacesaria²², C. Santamarina Rios³⁴, R. Santinelli³⁵, E. Santovetti^{21,k}, M. Sapunov⁶,
 A. Sarti^{18,l}, C. Satriano^{22,m}, A. Satta²¹, M. Savrie^{16,e}, D. Savrina²⁸, P. Schaack⁵⁰, M. Schiller³⁹,
 H. Schindler³⁵, S. Schleich⁹, M. Schlupp⁹, M. Schmelling¹⁰, B. Schmidt³⁵, O. Schneider³⁶,
 A. Schopper³⁵, M.-H. Schune⁷, R. Schwemmer³⁵, B. Sciascia¹⁸, A. Sciubba^{18,l}, M. Seco³⁴,
 A. Semennikov²⁸, K. Senderowska²⁴, I. Sepp⁵⁰, N. Serra³⁷, J. Serrano⁶, P. Seyfert¹¹,
 M. Shapkin³², I. Shapoval^{40,35}, P. Shatalov²⁸, Y. Shcheglov²⁷, T. Shears⁴⁹, L. Shekhtman³¹,
 O. Shevchenko⁴⁰, V. Shevchenko²⁸, A. Shires⁵⁰, R. Silva Coutinho⁴⁵, T. Skwarnicki⁵³,
 N.A. Smith⁴⁹, E. Smith^{52,46}, M. Smith⁵¹, K. Sobczak⁵, F.J.P. Soler⁴⁸, A. Solomin⁴³,
 F. Soomro^{18,35}, D. Souza⁴³, B. Souza De Paula², B. Spaan⁹, A. Sparkes⁴⁷, P. Spradlin⁴⁸,
 F. Stagni³⁵, S. Stahl¹¹, O. Steinkamp³⁷, S. Stoica²⁶, S. Stone⁵³, B. Storaci³⁸, M. Straticiu²⁶,

U. Straumann³⁷, V.K. Subbiah³⁵, S. Swientek⁹, M. Szczekowski²⁵, P. Szczypka^{36,35},
T. Szumlak²⁴, S. T'Jampens⁴, M. Teklishyn⁷, E. Teodorescu²⁶, F. Teubert³⁵, C. Thomas⁵²,
E. Thomas³⁵, J. van Tilburg¹¹, V. Tisserand⁴, M. Tobin³⁷, S. Tolks³⁹, S. Topp-Joergensen⁵²,
N. Torr⁵², E. Tournefier^{4,50}, S. Tourneur³⁶, M.T. Tran³⁶, A. Tsaregorodtsev⁶, N. Tuning³⁸,
M. Ubeda Garcia³⁵, A. Ukleja²⁵, U. Uwer¹¹, V. Vagnoni¹⁴, G. Valenti¹⁴, R. Vazquez Gomez³³,
P. Vazquez Regueiro³⁴, S. Vecchi¹⁶, J.J. Velthuis⁴³, M. Veltri^{17,9}, G. Veneziano³⁶,
M. Vesterinen³⁵, B. Viaud⁷, I. Videau⁷, D. Vieira², X. Vilasis-Cardona^{33,n}, J. Visniakov³⁴,
A. Vollhardt³⁷, D. Volyanskyy¹⁰, D. Voong⁴³, A. Vorobyev²⁷, V. Vorobyev³¹, C. Voß⁵⁵,
H. Voss¹⁰, R. Waldi⁵⁵, R. Wallace¹², S. Wandernoth¹¹, J. Wang⁵³, D.R. Ward⁴⁴, N.K. Watson⁴²,
A.D. Webber⁵¹, D. Websdale⁵⁰, M. Whitehead⁴⁵, J. Wicht³⁵, D. Wiedner¹¹, L. Wiggers³⁸,
G. Wilkinson⁵², M.P. Williams^{45,46}, M. Williams⁵⁰, F.F. Wilson⁴⁶, J. Wishahi⁹, M. Witek²³,
W. Witzeling³⁵, S.A. Wotton⁴⁴, S. Wright⁴⁴, S. Wu³, K. Wyllie³⁵, Y. Xie⁴⁷, F. Xing⁵², Z. Xing⁵³,
Z. Yang³, R. Young⁴⁷, X. Yuan³, O. Yushchenko³², M. Zangoli¹⁴, M. Zavertyaev^{10,a}, F. Zhang³,
L. Zhang⁵³, W.C. Zhang¹², Y. Zhang³, A. Zhelezov¹¹, L. Zhong³, A. Zvyagin³⁵.

¹ *Centro Brasileiro de Pesquisas Físicas (CBPF), Rio de Janeiro, Brazil*

² *Universidade Federal do Rio de Janeiro (UFRJ), Rio de Janeiro, Brazil*

³ *Center for High Energy Physics, Tsinghua University, Beijing, China*

⁴ *LAPP, Université de Savoie, CNRS/IN2P3, Annecy-Le-Vieux, France*

⁵ *Clermont Université, Université Blaise Pascal, CNRS/IN2P3, LPC, Clermont-Ferrand, France*

⁶ *CPPM, Aix-Marseille Université, CNRS/IN2P3, Marseille, France*

⁷ *LAL, Université Paris-Sud, CNRS/IN2P3, Orsay, France*

⁸ *LPNHE, Université Pierre et Marie Curie, Université Paris Diderot, CNRS/IN2P3, Paris, France*

⁹ *Fakultät Physik, Technische Universität Dortmund, Dortmund, Germany*

¹⁰ *Max-Planck-Institut für Kernphysik (MPIK), Heidelberg, Germany*

¹¹ *Physikalisches Institut, Ruprecht-Karls-Universität Heidelberg, Heidelberg, Germany*

¹² *School of Physics, University College Dublin, Dublin, Ireland*

¹³ *Sezione INFN di Bari, Bari, Italy*

¹⁴ *Sezione INFN di Bologna, Bologna, Italy*

¹⁵ *Sezione INFN di Cagliari, Cagliari, Italy*

¹⁶ *Sezione INFN di Ferrara, Ferrara, Italy*

¹⁷ *Sezione INFN di Firenze, Firenze, Italy*

¹⁸ *Laboratori Nazionali dell'INFN di Frascati, Frascati, Italy*

¹⁹ *Sezione INFN di Genova, Genova, Italy*

²⁰ *Sezione INFN di Milano Bicocca, Milano, Italy*

²¹ *Sezione INFN di Roma Tor Vergata, Roma, Italy*

²² *Sezione INFN di Roma La Sapienza, Roma, Italy*

²³ *Henryk Niewodniczanski Institute of Nuclear Physics Polish Academy of Sciences, Kraków, Poland*

²⁴ *AGH University of Science and Technology, Kraków, Poland*

²⁵ *National Center for Nuclear Research (NCBJ), Warsaw, Poland*

²⁶ *Horia Hulubei National Institute of Physics and Nuclear Engineering, Bucharest-Magurele, Romania*

²⁷ *Petersburg Nuclear Physics Institute (PNPI), Gatchina, Russia*

²⁸ *Institute of Theoretical and Experimental Physics (ITEP), Moscow, Russia*

²⁹ *Institute of Nuclear Physics, Moscow State University (SINP MSU), Moscow, Russia*

³⁰ *Institute for Nuclear Research of the Russian Academy of Sciences (INR RAN), Moscow, Russia*

³¹ *Budker Institute of Nuclear Physics (SB RAS) and Novosibirsk State University, Novosibirsk, Russia*

³² *Institute for High Energy Physics (IHEP), Protvino, Russia*

³³ *Universitat de Barcelona, Barcelona, Spain*

³⁴ *Universidad de Santiago de Compostela, Santiago de Compostela, Spain*

³⁵ *European Organization for Nuclear Research (CERN), Geneva, Switzerland*

- ³⁶ *Ecole Polytechnique Fédérale de Lausanne (EPFL), Lausanne, Switzerland*
- ³⁷ *Physik-Institut, Universität Zürich, Zürich, Switzerland*
- ³⁸ *Nikhef National Institute for Subatomic Physics, Amsterdam, The Netherlands*
- ³⁹ *Nikhef National Institute for Subatomic Physics and VU University Amsterdam, Amsterdam, The Netherlands*
- ⁴⁰ *NSC Kharkiv Institute of Physics and Technology (NSC KIPT), Kharkiv, Ukraine*
- ⁴¹ *Institute for Nuclear Research of the National Academy of Sciences (KINR), Kyiv, Ukraine*
- ⁴² *University of Birmingham, Birmingham, United Kingdom*
- ⁴³ *H.H. Wills Physics Laboratory, University of Bristol, Bristol, United Kingdom*
- ⁴⁴ *Cavendish Laboratory, University of Cambridge, Cambridge, United Kingdom*
- ⁴⁵ *Department of Physics, University of Warwick, Coventry, United Kingdom*
- ⁴⁶ *STFC Rutherford Appleton Laboratory, Didcot, United Kingdom*
- ⁴⁷ *School of Physics and Astronomy, University of Edinburgh, Edinburgh, United Kingdom*
- ⁴⁸ *School of Physics and Astronomy, University of Glasgow, Glasgow, United Kingdom*
- ⁴⁹ *Oliver Lodge Laboratory, University of Liverpool, Liverpool, United Kingdom*
- ⁵⁰ *Imperial College London, London, United Kingdom*
- ⁵¹ *School of Physics and Astronomy, University of Manchester, Manchester, United Kingdom*
- ⁵² *Department of Physics, University of Oxford, Oxford, United Kingdom*
- ⁵³ *Syracuse University, Syracuse, NY, United States*
- ⁵⁴ *Pontificia Universidade Católica do Rio de Janeiro (PUC-Rio), Rio de Janeiro, Brazil, associated to ²*
- ⁵⁵ *Institut für Physik, Universität Rostock, Rostock, Germany, associated to ¹¹*
- ^a *P.N. Lebedev Physical Institute, Russian Academy of Science (LPI RAS), Moscow, Russia*
- ^b *Università di Bari, Bari, Italy*
- ^c *Università di Bologna, Bologna, Italy*
- ^d *Università di Cagliari, Cagliari, Italy*
- ^e *Università di Ferrara, Ferrara, Italy*
- ^f *Università di Firenze, Firenze, Italy*
- ^g *Università di Urbino, Urbino, Italy*
- ^h *Università di Modena e Reggio Emilia, Modena, Italy*
- ⁱ *Università di Genova, Genova, Italy*
- ^j *Università di Milano Bicocca, Milano, Italy*
- ^k *Università di Roma Tor Vergata, Roma, Italy*
- ^l *Università di Roma La Sapienza, Roma, Italy*
- ^m *Università della Basilicata, Potenza, Italy*
- ⁿ *LIFAEELS, La Salle, Universitat Ramon Llull, Barcelona, Spain*
- ^o *Hanoi University of Science, Hanoi, Viet Nam*

1 Introduction

The ratio of Cabibbo-Kobayashi-Maskawa matrix [1] elements $|V_{td}|/|V_{ts}|$ has been measured in B mixing processes, where it is probed in box diagrams through the ratio of B^0 and B_s^0 mixing frequencies [2–5]. The ratio of these matrix elements has also been measured using the ratio of branching fractions of $b \rightarrow s\gamma$ and $b \rightarrow d\gamma$ decays, where radiative penguin diagrams mediate the transition [6–8]. These measurements of $|V_{td}|/|V_{ts}|$ are consistent, within the (dominant) $\sim 10\%$ uncertainty on the determination from radiative decays. The decays $b \rightarrow s\mu^+\mu^-$ and $b \rightarrow d\mu^+\mu^-$ offer an alternative way of measuring $|V_{td}|/|V_{ts}|$ which is sensitive to different classes of operators than the radiative decay modes [9]. These $b \rightarrow (s, d)\mu^+\mu^-$ transitions are flavour-changing neutral current processes which are forbidden at tree level in the Standard Model (SM). In the SM, the branching fractions for $b \rightarrow d\ell^+\ell^-$ transitions are suppressed relative to $b \rightarrow s\ell^+\ell^-$ processes by the ratio $|V_{td}|^2/|V_{ts}|^2$. This suppression does not necessarily apply to models beyond the SM, and $B^+ \rightarrow \pi^+\mu^+\mu^-$ decays¹ may be more sensitive to the effect of new particles than $B^+ \rightarrow K^+\mu^+\mu^-$ decays. In the SM, the ratio of branching fractions for these exclusive modes

$$R \equiv \mathcal{B}(B^+ \rightarrow \pi^+\mu^+\mu^-) / \mathcal{B}(B^+ \rightarrow K^+\mu^+\mu^-) \quad (1)$$

is given by $R = V^2 f^2$, where $V = |V_{td}|/|V_{ts}|$ and f is the ratio of the relevant form factors and Wilson coefficients, integrated over the relevant phase space. A difference between the measured value of R and $V^2 f^2$ would indicate a deviation from the minimal flavour violation hypothesis [10, 11], and would rule out certain approximate flavour symmetry models [12].

No $b \rightarrow d\ell^+\ell^-$ transitions have previously been detected, and the observation of the $B^+ \rightarrow \pi^+\mu^+\mu^-$ decay would therefore be the first time such a process has been seen. The predicted SM branching fraction for $B^+ \rightarrow \pi^+\mu^+\mu^-$ is $(2.0 \pm 0.2) \times 10^{-8}$ [13]. The most stringent limit to date is $\mathcal{B}(B^+ \rightarrow \pi^+\mu^+\mu^-) < 6.9 \times 10^{-8}$ at 90% confidence level [14]. The analogous $b \rightarrow s\ell^+\ell^-$ decay, $B^+ \rightarrow K^+\mu^+\mu^-$, has been observed with a branching fraction of $(4.36 \pm 0.15 \pm 0.18) \times 10^{-7}$ [15].

This paper describes the search for the $B^+ \rightarrow \pi^+\mu^+\mu^-$ decay using pp collision data, corresponding to an integrated luminosity of 1.0 fb^{-1} , collected with the LHCb detector. The $B^+ \rightarrow \pi^+\mu^+\mu^-$ branching fraction is measured with respect to that of $B^+ \rightarrow J/\psi(\rightarrow \mu^+\mu^-)K^+$, and the ratio of $B^+ \rightarrow \pi^+\mu^+\mu^-$ and $B^+ \rightarrow K^+\mu^+\mu^-$ branching fractions is also determined.

The LHCb detector [16] is a single-arm forward spectrometer covering the pseudo-rapidity range $2 < \eta < 5$. The experiment is designed for the study of particles containing b or c quarks. The apparatus includes a high precision tracking system, consisting of a silicon-strip vertex detector surrounding the pp interaction region, and a large-area silicon-strip detector located upstream of a dipole magnet. The dipole magnet has a bending power of about 4 Tm. Three stations of silicon-strip detectors and straw drift-tubes are placed downstream of the magnet. The combined tracking system has a momentum resolution

¹Charge conjugation is implicit throughout this paper.

40 $\Delta p/p$ that varies from 0.4% at momenta of 5 GeV/c, to 0.6% at 100 GeV/c. The tracking
 41 system gives an impact parameter resolution of 20 μm for tracks with a high transverse
 42 momentum (p_T). Charged hadrons are identified using two ring-imaging Cherenkov
 43 detectors. Photon, electron and hadron candidates are identified by a calorimeter system
 44 consisting of scintillating-pad and preshower detectors, an electromagnetic calorimeter and
 45 a hadronic calorimeter. Muons are identified by a system composed of alternating layers
 46 of iron and either multi-wire proportional chambers or triple gaseous electron multipliers.

47 In the present analysis, events are first required to have passed a hardware trigger
 48 which selects high- p_T single muons or dimuons. In the first stage of the subsequent software
 49 trigger, a single high impact parameter and high- p_T track is required. In the second stage
 50 of the software trigger, events are reconstructed and then selected for storage based on
 51 either the (partially) reconstructed B candidate or the dimuon candidate [17, 18].

52 To produce simulated samples of signal and background decays, pp collisions are
 53 generated using PYTHIA 6.4 [19] with a specific LHCb configuration [20]. Decays of
 54 hadronic particles are described by the EVTGEN package [21] in which final state radiation
 55 is generated using PHOTOS [22]. The interaction of the generated particles with the
 56 detector and the detector response are implemented using the GEANT4 toolkit [23], as
 57 described in Ref. [24].

58 The small branching fractions of the $B^+ \rightarrow \pi^+ \mu^+ \mu^-$ and $B^+ \rightarrow K^+ \mu^+ \mu^-$ signal decays
 59 necessitate good control of the backgrounds and the use of suitably constrained models to
 60 fit the invariant-mass distributions. The decay $B^+ \rightarrow J/\psi (\rightarrow \mu^+ \mu^-) K^+$ (hereafter denoted
 61 $B^+ \rightarrow J/\psi K^+$) is used to extract both the shape of the signal mass peaks and, in the
 62 $B^+ \rightarrow \pi^+ \mu^+ \mu^-$ case, the invariant mass distribution of the misidentified $B^+ \rightarrow K^+ \mu^+ \mu^-$
 63 events. These misidentified $B^+ \rightarrow K^+ \mu^+ \mu^-$ events form the main residual background
 64 after the application of the selection requirements.

65 2 Event selection

66 The $B^+ \rightarrow \pi^+ \mu^+ \mu^-$ and $B^+ \rightarrow K^+ \mu^+ \mu^-$ candidates are selected by combining pairs of
 67 oppositely charged muons with a charged pion or kaon. The selection includes requirements
 68 on the impact parameters of the final-state particles and B candidate, the vertex quality
 69 and displacement of the B candidate, particle identification (PID) requirements on the
 70 muons and a requirement that the B candidate momentum vector points to one of the
 71 primary vertices in the event. The rate of events containing more than one reconstructed
 72 candidate is 1 in $\sim 20,000$ for $B^+ \rightarrow J/\psi K^+$. No restriction is therefore placed on the
 73 number of candidates per event.

74 The pion identification requirements select a sample of pions with an efficiency of $\sim 70\%$
 75 and a kaon rejection of 99%. The kaon identification requirements allow the selection of a
 76 mutually exclusive sample with similar efficiencies. The muon identification requirements
 77 have an efficiency of $\sim 80\%$, with a pion rejection of $\sim 99.5\%$. The PID requirements have
 78 a momentum dependent efficiency which is measured from data, in bins of momentum,
 79 pseudorapidity and track multiplicity. The efficiency of the hadron PID requirements is

80 measured from a sample of $D^{*+} \rightarrow (D^0 \rightarrow K^- \pi^+) \pi^+$ candidates that allows the hadrons
 81 to be unambiguously identified based on their kinematics. The muon PID efficiencies are
 82 measured using $B^+ \rightarrow J/\psi K^+$ candidates, using a tag and probe method.

83 The J/ψ and $\psi(2S)$ resonances, where $J/\psi, \psi(2S) \rightarrow \mu^+ \mu^-$, are excluded using a
 84 veto on the dimuon mass. This veto has a total width of 200 (150) MeV/c^2 around the
 85 nominal J/ψ ($\psi(2S)$) mass [25], and takes into account the radiative tail of these decays.
 86 Candidates where the dimuon mass is poorly measured have a correlated mismeasurement
 87 in the $h\mu\mu$ mass. The veto therefore includes a component which shifts with $h\mu\mu$ mass
 88 to exclude such candidates. Several other backgrounds are considered: combinatorial
 89 backgrounds, where the particles selected do not originate from a single decay; peaking
 90 backgrounds, where a single decay is selected but with one or more particles misidentified;
 91 and partially reconstructed backgrounds, where one or more final-state particles from a B
 92 decay are not reconstructed. These backgrounds are each described below.

93 2.1 Combinatorial backgrounds

94 A boosted decision tree (BDT) [26] which employs the AdaBoost algorithm [27] is used to
 95 separate signal candidates from the combinatorial background. Kinematic and geometric
 96 properties of the B^+ candidate and final state particles, B^+ candidate vertex quality and
 97 final state particle track quality are input variables to the BDT.

98 The BDT is trained on a simulated $B^+ \rightarrow \pi^+ \mu^+ \mu^-$ signal sample, and a background
 99 sample taken from sidebands in the $B^+ \rightarrow \pi^+ \mu^+ \mu^-$ and $B^+ \rightarrow K^+ \mu^+ \mu^-$ invariant
 100 mass distributions. These invariant masses are denoted $M_{\pi^+ \mu^+ \mu^-}$ and $M_{K^+ \mu^+ \mu^-}$, re-
 101 spectively. The background sample consists of 20% of the candidates with $M_{\pi^+ \mu^+ \mu^-}$ or
 102 $M_{K^+ \mu^+ \mu^-} > 5500 \text{ MeV}/c^2$. This sample is not used for any of the subsequent analysis.
 103 Signal candidates are required to have a BDT output which exceeds a set value. This
 104 value is determined by simulating an ensemble of datasets with the expected signal and
 105 background yields, and choosing the cut value which gives the best statistical significance
 106 for the $B^+ \rightarrow \pi^+ \mu^+ \mu^-$ signal yield. The same method is used to select the optimal set
 107 of PID requirements. The BDT output distribution for simulated $B^+ \rightarrow \pi^+ \mu^+ \mu^-$ events
 108 and for mass sideband candidates is shown in Fig. 1. A cut on the BDT output > 0.325
 109 reduces the expected combinatorial background from 652 ± 11 to 9 ± 2 candidates in a
 110 $\pm 60 \text{ MeV}/c^2$ window around the nominal B mass, while retaining 68% of signal events.
 111 Assuming the SM branching fraction and the single event sensitivity defined in Sect. 4,
 112 21 ± 3 $B^+ \rightarrow \pi^+ \mu^+ \mu^-$ signal events are expected in the data sample.

113 2.2 Peaking and partially reconstructed backgrounds

114 Backgrounds from fully reconstructed B^+ decays with one or more misidentified parti-
 115 cles have a peaking mass structure. After applying the PID requirements, the fraction
 116 of $B^+ \rightarrow K^+ \mu^+ \mu^-$ candidates misidentified as $B^+ \rightarrow \pi^+ \mu^+ \mu^-$ is 0.9%, giving a resid-
 117 ual background expectation of 6.2 ± 0.3 candidates. This expectation is computed by
 118 weighting $B^+ \rightarrow K^+ \mu^+ \mu^-$ candidates, isolated using a kaon PID requirement, accord-

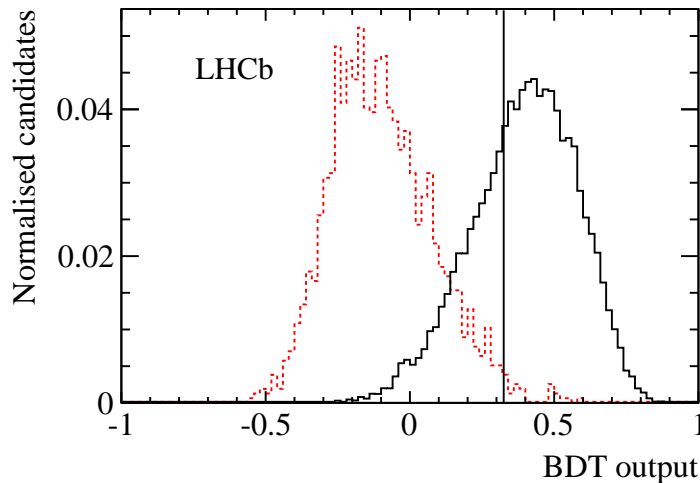


Figure 1: BDT output distribution for simulated $B^+ \rightarrow \pi^+ \mu^+ \mu^-$ events (black solid line) and candidates taken from the mass sidebands in the data (red dotted line). Both distributions are normalised to unit area. The vertical line indicates the chosen cut value of 0.325.

119 ing to the PID efficiency obtained from the D^{*+} calibration sample. The only other
 120 decay found to give a significant peaking background in the search for $B^+ \rightarrow \pi^+ \mu^+ \mu^-$ is
 121 $B^+ \rightarrow \pi^+ \pi^+ \pi^-$, where both a π^+ and a π^- are misidentified as muons. For $B^+ \rightarrow K^+ \mu^+ \mu^-$
 122 decays, the only significant peaking background is $B^+ \rightarrow K^+ \pi^+ \pi^-$, which includes
 123 the contribution from $B^+ \rightarrow \bar{D}^0 (\rightarrow K^+ \pi^-) \pi^+$. The expected background levels from
 124 $B^+ \rightarrow \pi^+ \pi^+ \pi^-$ ($B^+ \rightarrow K^+ \pi^+ \pi^-$) decays are computed to be 0.39 ± 0.04 (1.56 ± 0.16)
 125 residual background candidates, using simulated events.

126 Backgrounds from decays that have one or more final state particles which are not
 127 reconstructed have a mass below the nominal B mass, and do not extend into the signal
 128 window. However, in the $B^+ \rightarrow \pi^+ \mu^+ \mu^-$ case, these backgrounds overlap with the
 129 misidentified $B^+ \rightarrow K^+ \mu^+ \mu^-$ component described above, and must therefore be included
 130 in the fit. In the $B^+ \rightarrow K^+ \mu^+ \mu^-$ case such partially reconstructed backgrounds are
 131 negligible.

132 2.3 Control channels

133 The $B^+ \rightarrow J/\psi K^+$ and $B^+ \rightarrow K^+ \mu^+ \mu^-$ decay candidates are isolated by replacing the pion
 134 PID criteria with a requirement to select kaons. In addition, instead of the dimuon mass
 135 vetoes described above, the $B^+ \rightarrow J/\psi K^+$ candidates are required to have dimuon mass
 136 within ± 50 MeV/ c^2 of the nominal J/ψ mass (the J/ψ mass resolution is 14.5 MeV/ c^2).
 137 The remainder of the selection is the same as that used for $B^+ \rightarrow \pi^+ \mu^+ \mu^-$. This minimises
 138 the systematic uncertainty on the ratio of branching fractions, although the selection
 139 is considerably tighter than that which would give the lowest statistical uncertainty

140 on the $B^+ \rightarrow K^+ \mu^+ \mu^-$ event yield. The $B^+ \rightarrow (J/\psi \rightarrow \mu^+ \mu^-) \pi^+$ candidates (denoted
 141 $B^+ \rightarrow J/\psi \pi^+$), which are discussed below, are selected using the same BDT, the pion PID
 142 criteria, and the above window on the dimuon invariant mass. There is no significant
 143 peaking background for $B^+ \rightarrow J/\psi K^+$ decays. For $B^+ \rightarrow J/\psi \pi^+$ decays the only significant
 144 peaking background is misidentified $B^+ \rightarrow J/\psi K^+$ events.

145 **3 Signal yield determination**

146 The $B^+ \rightarrow \pi^+ \mu^+ \mu^-$, $B^+ \rightarrow K^+ \mu^+ \mu^-$ and $B^+ \rightarrow J/\psi K^+$ yields are determined from a
 147 simultaneous unbinned maximum likelihood fit to four invariant mass distributions which
 148 contain:

- 149 1. Reconstructed $B^+ \rightarrow J/\psi K^+$ candidates;
- 150 2. Reconstructed $B^+ \rightarrow J/\psi K^+$ candidates, with the kaon attributed to have the pion
 151 mass;
- 152 3. Reconstructed $B^+ \rightarrow \pi^+ \mu^+ \mu^-$ candidates; and
- 153 4. Reconstructed $B^+ \rightarrow K^+ \mu^+ \mu^-$ candidates.

154 The signal probability density functions (PDFs) for the $B^+ \rightarrow \pi^+ \mu^+ \mu^-$, $B^+ \rightarrow K^+ \mu^+ \mu^-$,
 155 and $B^+ \rightarrow J/\psi K^+$ decay modes are modelled with the sum of two Gaussian functions.
 156 The PDFs for all of these decay modes share the same mean, widths and fraction of
 157 the total PDF between the two Gaussians. The $B^+ \rightarrow \pi^+ \mu^+ \mu^-$ PDF is adjusted for the
 158 difference between the widths of the $B^+ \rightarrow \pi^+ \mu^+ \mu^-$ and $B^+ \rightarrow J/\psi K^+$ distributions, which
 159 is observed to be at the percent level in simulation. The peaking backgrounds described
 160 in Sect. 2.2 are taken into account in the fit by including PDFs with shapes determined
 161 from simulation. The combinatorial backgrounds are modelled with a single exponential
 162 PDF, with the exponent allowed to vary independently for each distribution. The partially
 163 reconstructed candidates are modelled using a PDF consisting of an exponential distribution
 164 cut-off at a threshold mass, with the transition smeared by the experimental resolution.
 165 The shape parameters are again allowed to vary independently for each distribution. The
 166 misidentified $B^+ \rightarrow J/\psi K^+$ candidates are modelled with a Crystal Ball function [28], as
 167 it describes the shape well. In order to describe the relevant background components for
 168 $B^+ \rightarrow \pi^+ \mu^+ \mu^-$, the fit is performed in the mass range $4900 < M_{\pi^+ \mu^+ \mu^-} < 7000$ MeV/ c^2 . To
 169 avoid fitting the partially reconstructed background for $B^+ \rightarrow K^+ \mu^+ \mu^-$, which is irrelevant
 170 for the analysis, the fit is performed in the mass range $5170 < M_{K^+ \mu^+ \mu^-} < 7000$ MeV/ c^2 .

171 **3.1 Reconstructed $B^+ \rightarrow J/\psi K^+$ candidates**

172 The reconstructed $B^+ \rightarrow J/\psi K^+$ candidates are shown in the $M_{K^+ \mu^+ \mu^-}$ distribution
 173 in Fig. 2(a). The fitted $B^+ \rightarrow J/\psi K^+$ yield is $106,230 \pm 330$. This large event yield
 174 determines the lineshape for the $B^+ \rightarrow \pi^+ \mu^+ \mu^-$ and $B^+ \rightarrow K^+ \mu^+ \mu^-$ signal distributions,
 175 and provides the normalisation for the $B^+ \rightarrow \pi^+ \mu^+ \mu^-$ branching fraction.

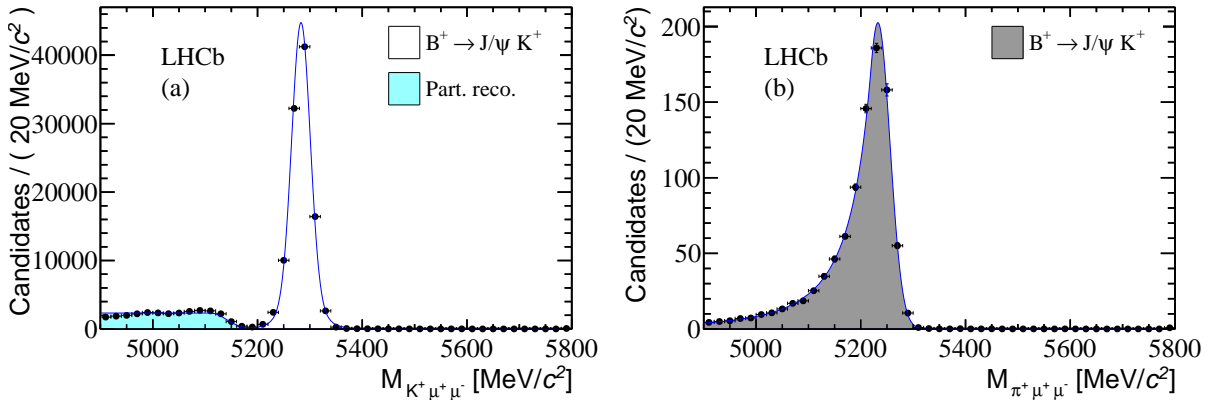


Figure 2: Invariant mass distribution for $B^+ \rightarrow J/\psi K^+$ candidates under the (a) $K^+ \mu^+ \mu^-$ and (b) $\pi^+ \mu^+ \mu^-$ mass hypotheses with the fit projections overlaid. In the legend, “part. reco” refers to partially reconstructed background. The fit models are described in the text.

176 3.2 Reconstructed $B^+ \rightarrow J/\psi K^+$ candidates with the pion mass 177 hypothesis

178 The $B^+ \rightarrow J/\psi K^+$ candidates reconstructed under the pion mass hypothesis provide
179 the lineshape for the misidentified $B^+ \rightarrow K^+ \mu^+ \mu^-$ candidates that are a background
180 to the $B^+ \rightarrow \pi^+ \mu^+ \mu^-$ signal. The equivalent background from $B^+ \rightarrow \pi^+ \mu^+ \mu^-$ in the
181 $B^+ \rightarrow K^+ \mu^+ \mu^-$ sample is negligible.

182 The PID requirements used in the selection have a momentum dependent efficiency
183 and therefore change the mass distribution of any backgrounds with candidates that have
184 misidentified particles. In order to correct for this effect, the $B^+ \rightarrow J/\psi K^+$ candidates are
185 reweighted according to the PID efficiencies derived from data, as described in Sect. 2.2.
186 This adjusts the $B^+ \rightarrow J/\psi K^+$ invariant mass distribution to remove the effect of the kaon
187 PID requirement used to isolate $B^+ \rightarrow J/\psi K^+$, and to reproduce the effect of the pion
188 PID requirement used to isolate $B^+ \rightarrow \pi^+ \mu^+ \mu^-$. In addition, there is a difference in the
189 lineshapes of the $B^+ \rightarrow J/\psi K^+$ and $B^+ \rightarrow K^+ \mu^+ \mu^-$ invariant mass distributions under the
190 pion mass hypothesis. This effect arises from the differences between the two decay modes’
191 dimuon energy and hadron momentum spectra, and is therefore corrected by reweighting
192 $B^+ \rightarrow J/\psi K^+$ candidates in terms of these variables. The $M_{\pi^+ \mu^+ \mu^-}$ distribution after both
193 weighting procedures have been applied is shown in Fig. 2(b).

194 3.3 Reconstructed $B^+ \rightarrow \pi^+ \mu^+ \mu^-$ and $B^+ \rightarrow K^+ \mu^+ \mu^-$ candi- 195 dates

196 The yield of misidentified $B^+ \rightarrow K^+ \mu^+ \mu^-$ candidates in the $B^+ \rightarrow \pi^+ \mu^+ \mu^-$ invariant mass
197 distribution is constrained to the expectation given in Sect. 2.2. Performing the fit without
198 this constraint gives a yield of 5.6 ± 6.4 misidentified $B^+ \rightarrow K^+ \mu^+ \mu^-$ candidates. The

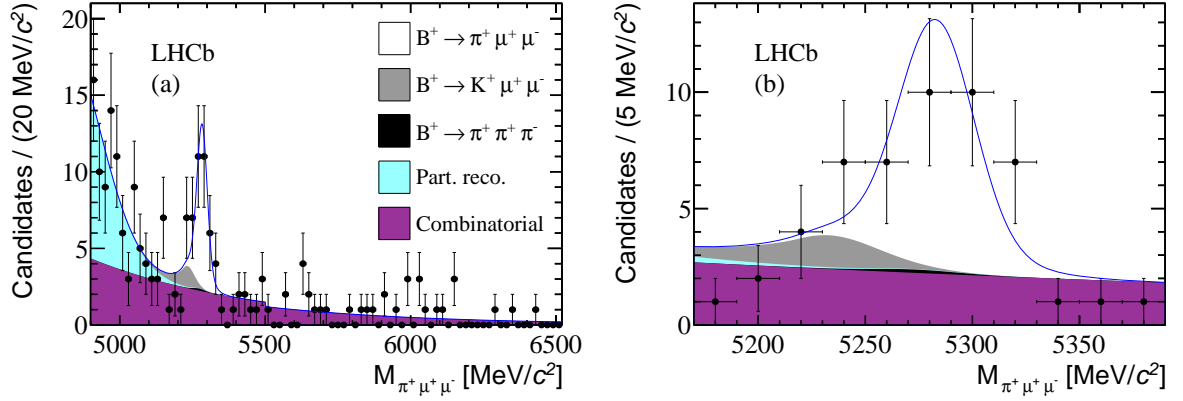


Figure 3: Invariant mass distribution of $B^+ \rightarrow \pi^+ \mu^+ \mu^-$ candidates with the fit projection overlaid (a) in the full mass range and (b) in the region around the B mass. In the legend, “part. reco.” and “combinatorial” refer to partially reconstructed and combinatorial backgrounds respectively. The discontinuity at 5500 MeV/c^2 is due to the removal of data used for training the BDT.

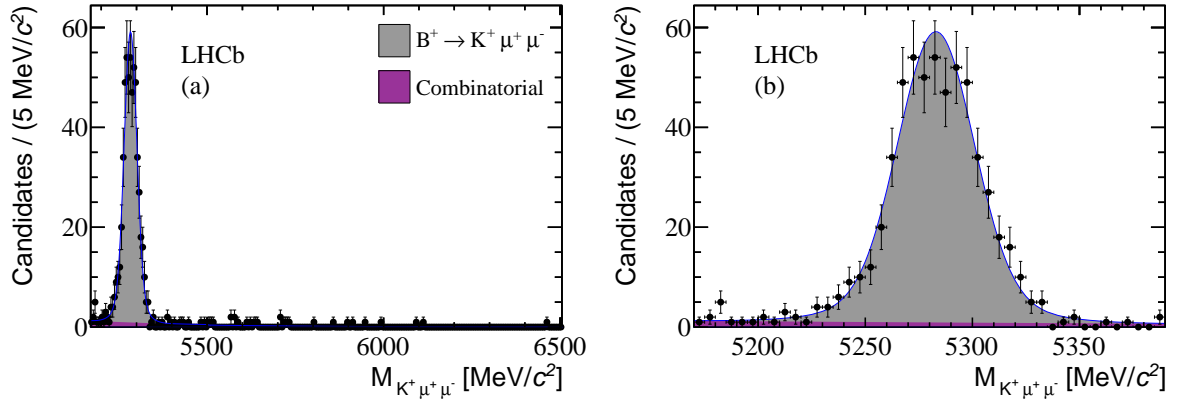


Figure 4: Invariant mass distribution of $B^+ \rightarrow K^+ \mu^+ \mu^-$ candidates with the fit projection overlaid (a) in the full mass range and (b) in the region around the B mass. In the legend, “combinatorial” refers to the combinatorial background.

199 yields for the peaking background components are constrained to the expectations given in
 200 Sect. 2.2. For both the $M_{\pi^+ \mu^+ \mu^-}$ and $M_{K^+ \mu^+ \mu^-}$ distributions, the exponential PDF used
 201 to model the combinatorial background has a step in the normalisation at 5500 MeV/c^2
 202 to account for the data used for training the BDT.

203 The $M_{\pi^+ \mu^+ \mu^-}$ and $M_{K^+ \mu^+ \mu^-}$ distributions are shown in Figs 3 and 4, respectively. The
 204 fit gives a $B^+ \rightarrow \pi^+ \mu^+ \mu^-$ signal yield of $25.3^{+6.7}_{-6.4}$, and a $B^+ \rightarrow K^+ \mu^+ \mu^-$ signal yield of
 205 553^{+24}_{-25} .

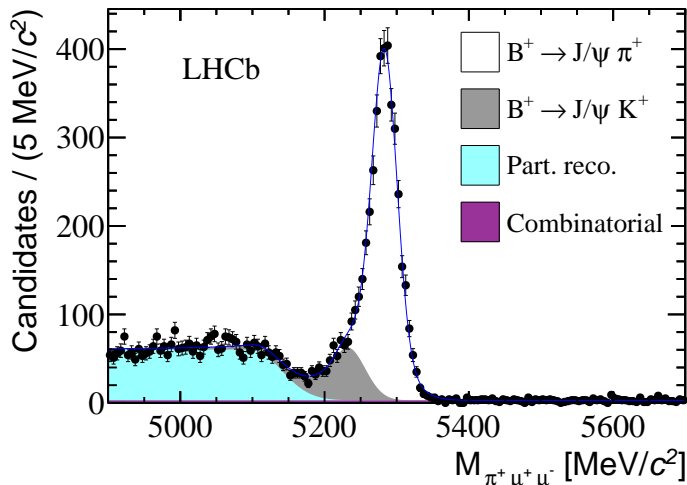


Figure 5: Invariant mass distribution of $B^+ \rightarrow J/\psi \pi^+$ candidates with the fit projection overlaid. In the legend, “part. reco.” and “combinatorial” refer to partially reconstructed and combinatorial backgrounds respectively. The fit model is described in the text.

206 3.4 Cross check of the fit procedure

207 The fit procedure was cross-checked on $B^+ \rightarrow J/\psi \pi^+$ decays, accounting for the background
 208 from $B^+ \rightarrow J/\psi K^+$ decays. The resulting fit is shown in Fig. 5. The shape of the combined
 209 $B^+ \rightarrow J/\psi \pi^+$ and $B^+ \rightarrow J/\psi K^+$ mass distribution is well reproduced. The $B^+ \rightarrow J/\psi K^+$
 210 yield is not constrained in this fit. The fitted yield of 1024 ± 61 candidates is consistent
 211 with the expectation of 958 ± 31 (stat.) candidates. This expectation is again computed by
 212 weighting the $B^+ \rightarrow J/\psi K^+$ candidates, which are isolated using a kaon PID requirement,
 213 according to the PID efficiency derived from $D^{*+} \rightarrow (D^0 \rightarrow K^- \pi^+) \pi^+$ events.

214 4 Determination of branching fractions

215 The $B^+ \rightarrow \pi^+ \mu^+ \mu^-$ branching fraction is given by

$$\mathcal{B}(B^+ \rightarrow \pi^+ \mu^+ \mu^-) = \frac{\mathcal{B}(B^+ \rightarrow J/\psi K^+)}{N_{B^+ \rightarrow J/\psi K^+}} \frac{\epsilon_{B^+ \rightarrow J/\psi K^+}}{\epsilon_{B^+ \rightarrow \pi^+ \mu^+ \mu^-}} N_{B^+ \rightarrow \pi^+ \mu^+ \mu^-} \quad (2)$$

$$= \alpha \cdot N_{B^+ \rightarrow \pi^+ \mu^+ \mu^-}, \quad (3)$$

216 where $\mathcal{B}(X)$, N_X and ϵ_X are the branching fraction, the number of events and the
 217 total efficiency, respectively, for decay mode X , and α is the single event sensitiv-
 218 ity. The total efficiency includes reconstruction, trigger and selection efficiencies. The
 219 ratio $\epsilon_{B^+ \rightarrow J/\psi K^+} / \epsilon_{B^+ \rightarrow \pi^+ \mu^+ \mu^-}$ is determined to be 1.60 ± 0.01 using simulated events,
 220 where the uncertainty is due to the limited sizes of the simulated samples only. Other
 221 sources of systematic uncertainty are discussed in Sect. 5. The difference in efficien-
 222 cies between $B^+ \rightarrow \pi^+ \mu^+ \mu^-$ and $B^+ \rightarrow J/\psi K^+$ events is largely due to the mass vetoes

223 used to remove the charmonium resonances, and the different PID requirements. The
 224 $B^+ \rightarrow J/\psi(\rightarrow \mu^+\mu^-)K^+$ branching fraction is $(6.02 \pm 0.20) \times 10^{-5}$ [25]. Together with the
 225 other quantities in Eq. 2, this gives a single event sensitivity of $\alpha = (9.1 \pm 0.1) \times 10^{-10}$,
 226 where the uncertainty is due to the limited sizes of the simulated samples only.

227 The ratio of $B^+ \rightarrow \pi^+\mu^+\mu^-$ and $B^+ \rightarrow K^+\mu^+\mu^-$ branching fractions is given by

$$R = \frac{N_{B^+ \rightarrow \pi^+\mu^+\mu^-}}{N_{B^+ \rightarrow K^+\mu^+\mu^-}} \frac{\epsilon_{B^+ \rightarrow K^+\mu^+\mu^-}}{\epsilon_{B^+ \rightarrow \pi^+\mu^+\mu^-}}, \quad (4)$$

228 where simulated events give $\epsilon_{B^+ \rightarrow K^+\mu^+\mu^-} / \epsilon_{B^+ \rightarrow \pi^+\mu^+\mu^-} = 1.15 \pm 0.01$.

229 5 Systematic uncertainties

230 Two sources of systematic uncertainties are considered: those affecting the determination
 231 of the $B^+ \rightarrow \pi^+\mu^+\mu^-$ and $B^+ \rightarrow K^+\mu^+\mu^-$ signal yields, and those affecting only the
 232 normalisation.

233 Uncertainties in the shape parameters for the misidentified $B^+ \rightarrow K^+\mu^+\mu^-$ PDF in
 234 the fit are taken into account by including Gaussian constraints on their values. The
 235 most significant sources of uncertainty in the determination of these shape parameters
 236 arise from the procedure for correcting the $B^+ \rightarrow J/\psi K^+$ mass shape to match that of
 237 the $B^+ \rightarrow K^+\mu^+\mu^-$ decay, and the correction for the hadron PID requirements. The
 238 uncertainty on the $B^+ \rightarrow \pi^+\mu^+\mu^-$ yield determined with the fit takes these shape parameter
 239 uncertainties into account, and they are therefore included in the statistical rather than
 240 the systematic uncertainty. These uncertainties affect the $B^+ \rightarrow \pi^+\mu^+\mu^-$ yield at below
 241 the one percent level. None of these effects give rise to any significant uncertainty for the
 242 $B^+ \rightarrow K^+\mu^+\mu^-$ decay.

243 Uncertainties on the two efficiency ratios $\epsilon_{B^+ \rightarrow J/\psi K^+} / \epsilon_{B^+ \rightarrow \pi^+\mu^+\mu^-}$ and
 244 $\epsilon_{B^+ \rightarrow K^+\mu^+\mu^-} / \epsilon_{B^+ \rightarrow \pi^+\mu^+\mu^-}$ affect the conversion of the $B^+ \rightarrow \pi^+\mu^+\mu^-$ yield into a
 245 branching fraction, and the measurement of the ratio of branching fractions R . The
 246 largest systematic uncertainty on these efficiency ratios is the choice of form factors used
 247 to generate the simulated events. Using an alternative set of form factors changes the
 248 $B^+ \rightarrow \pi^+\mu^+\mu^-$ efficiency by 3%, and this difference is taken as a systematic uncertainty.
 249 For the ratio of $B^+ \rightarrow \pi^+\mu^+\mu^-$ and $B^+ \rightarrow K^+\mu^+\mu^-$, the alternative form factors are used
 250 for both $B^+ \rightarrow \pi^+\mu^+\mu^-$ and $B^+ \rightarrow K^+\mu^+\mu^-$, giving a systematic uncertainty of 1.7%.
 251 To estimate the uncertainty arising from the PID efficiency, the ratio of corrected yields
 252 between the $B^+ \rightarrow J/\psi K^+$ and $B^+ \rightarrow J/\psi \pi^+$ decay modes is measured, varying the PID
 253 requirements. The largest resulting difference with respect to the nominal value is 1.1%,
 254 which is taken as the systematic uncertainty.

255 The systematic uncertainty arising from the knowledge of the trigger efficiency is
 256 determined using $B^+ \rightarrow J/\psi K^+$ candidates in the data. Taking the events which pass
 257 the trigger independently of the $B^+ \rightarrow J/\psi K^+$ candidate, the fraction of these events
 258 which also pass the trigger based on the $B^+ \rightarrow J/\psi K^+$ candidate provides a determination
 259 of the trigger efficiency. The efficiency determined in this way is compared to that

Table 1: Summary of systematic uncertainties.

Source	$\mathcal{B}(B^+ \rightarrow \pi^+ \mu^+ \mu^-)$ (%)	$\frac{\mathcal{B}(B^+ \rightarrow \pi^+ \mu^+ \mu^-)}{\mathcal{B}(B^+ \rightarrow K^+ \mu^+ \mu^-)}$ (%)
Form factors	3.0	1.7
Trigger efficiency	1.4	1.4
PID performance	1.1	1.1
Data simulation differences	0.4	0.4
Simulation sample size	0.7	0.7
$\mathcal{B}(B^+ \rightarrow J/\psi (\rightarrow \mu^+ \mu^-) K^+)$	3.5	–
Total	5.0	2.6

260 calculated in simulated events using the same method, and the difference is taken as
 261 the systematic uncertainty. This gives a 1.4% uncertainty on $\epsilon_{B^+ \rightarrow J/\psi K^+} / \epsilon_{B^+ \rightarrow \pi^+ \mu^+ \mu^-}$ and
 262 $\epsilon_{B^+ \rightarrow K^+ \mu^+ \mu^-} / \epsilon_{B^+ \rightarrow \pi^+ \mu^+ \mu^-}$.

263 For all decays under consideration, there are small differences between the distributions
 264 of some reconstructed quantities in the data and in the simulated events. These differences
 265 are assessed by comparing the distributions of data and simulated events for $B^+ \rightarrow J/\psi K^+$
 266 candidates. The simulation is corrected to match the data where it disagrees, and the
 267 resulting 0.4% difference between the raw and corrected ratio of $B^+ \rightarrow J/\psi K^+$ and
 268 $B^+ \rightarrow \pi^+ \mu^+ \mu^-$ efficiencies is taken as a systematic uncertainty. The statistical uncertainty
 269 from the limited simulation sample size is 0.7%. When normalising to $B^+ \rightarrow J/\psi K^+$, the
 270 measured $B^+ \rightarrow J/\psi K^+$ and $J/\psi \rightarrow \mu^+ \mu^-$ branching fractions contribute an uncertainty
 271 of 3.5% to the $B^+ \rightarrow \pi^+ \mu^+ \mu^-$ branching fraction. The systematic uncertainties are
 272 summarised in Table 1.

273 6 Results and conclusion

274 The statistical significance of the $B^+ \rightarrow \pi^+ \mu^+ \mu^-$ signal observed in Fig. 3 is computed
 275 from the difference in the minimum log-likelihood between the signal-plus-background
 276 and background-only hypotheses. Both the statistical and systematic uncertainties on
 277 the shape parameters (which affect the significance) are taken into account. The fitted
 278 yield corresponds to an observation of the $B^+ \rightarrow \pi^+ \mu^+ \mu^-$ decay with 5.2σ significance.
 279 This is the first observation of a $b \rightarrow d \ell^+ \ell^-$ transition. Normalising the observed signal to
 280 the $B^+ \rightarrow J/\psi K^+$ decay, using the single event sensitivity given in Sect. 4, the branching
 281 fraction of the $B^+ \rightarrow \pi^+ \mu^+ \mu^-$ decay is measured to be

$$\mathcal{B}(B^+ \rightarrow \pi^+ \mu^+ \mu^-) = (2.3 \pm 0.6 \text{ (stat.)} \pm 0.1 \text{ (syst.)}) \times 10^{-8}.$$

282 This is compatible with the SM expectation of $(2.0 \pm 0.2) \times 10^{-8}$ [13]. Given the agreement
 283 between the present measurement and the SM prediction, contributions from physics
 284 beyond the SM can only modify the $B^+ \rightarrow \pi^+ \mu^+ \mu^-$ branching fraction by a small amount.
 285 A significant improvement in the precision of both the experimental measurements and the
 286 theoretical prediction will therefore be required to resolve any new physics contributions.

287 Taking the measured $B^+ \rightarrow K^+ \mu^+ \mu^-$ yield and $\epsilon_{B^+ \rightarrow K^+ \mu^+ \mu^-} / \epsilon_{B^+ \rightarrow \pi^+ \mu^+ \mu^-}$, the ratio of
 288 $B^+ \rightarrow \pi^+ \mu^+ \mu^-$ and $B^+ \rightarrow K^+ \mu^+ \mu^-$ branching fractions is measured to be

$$\frac{\mathcal{B}(B^+ \rightarrow \pi^+ \mu^+ \mu^-)}{\mathcal{B}(B^+ \rightarrow K^+ \mu^+ \mu^-)} = 0.053 \pm 0.014 \text{ (stat.)} \pm 0.001 \text{ (syst.)}.$$

289 In order to extract $|V_{td}|/|V_{ts}|$ from this ratio of branching fractions, the SM expectation
 290 for the ratio of $B^+ \rightarrow \pi^+ \mu^+ \mu^-$ and $B^+ \rightarrow K^+ \mu^+ \mu^-$ branching fractions is calculated using
 291 the EVTGEN package [21], which implements the calculation in Ref. [29]. This calculation
 292 has been updated with the expressions for Wilson coefficients and power corrections from
 293 Ref. [30], and formulae for the q^2 dependence of these coefficients from Refs. [31, 32].
 294 Using this calculation, and form factors taken from Ref. [33] (“set II”), the integrated
 295 ratio of form factors and Wilson coefficients is determined to be $f = 0.87$. Neglecting
 296 theoretical uncertainties, the measured ratio of $B^+ \rightarrow \pi^+ \mu^+ \mu^-$ and $B^+ \rightarrow K^+ \mu^+ \mu^-$
 297 branching fractions then gives

$$|V_{td}|/|V_{ts}| = \frac{1}{f} \sqrt{\frac{\mathcal{B}(B^+ \rightarrow \pi^+ \mu^+ \mu^-)}{\mathcal{B}(B^+ \rightarrow K^+ \mu^+ \mu^-)}} = 0.266 \pm 0.035 \text{ (stat.)} \pm 0.003 \text{ (syst.)},$$

298 which is compatible with previous determinations [5–8]. An additional uncertainty will arise
 299 from the knowledge of the form factors. As an estimate of the scale of this uncertainty,
 300 the “set IV” parameters available in Ref. [33] change the value of $|V_{td}|/|V_{ts}|$ by 5.1%.
 301 This estimate is unlikely to cover a one sigma range on the form factor uncertainty, and
 302 does not take into account additional sources of uncertainty beyond the form factors.
 303 A full theoretical calculation taking into account such additional uncertainties, which
 304 also accurately determines the uncertainty on the ratio of form factors, would allow a
 305 determination of $|V_{td}|/|V_{ts}|$ with comparable precision to that from radiative penguin
 306 decays.

307 Acknowledgements

308 We express our gratitude to our colleagues in the CERN accelerator departments for the
 309 excellent performance of the LHC. We thank the technical and administrative staff at
 310 CERN and at the LHCb institutes, and acknowledge support from the National Agencies:
 311 CAPES, CNPq, FAPERJ and FINEP (Brazil); CERN; NSFC (China); CNRS/IN2P3
 312 (France); BMBF, DFG, HGF and MPG (Germany); SFI (Ireland); INFN (Italy); FOM
 313 and NWO (The Netherlands); SCSR (Poland); ANCS (Romania); MinES of Russia
 314 and Rosatom (Russia); MICINN, XuntaGal and GENCAT (Spain); SNSF and SER
 315 (Switzerland); NAS Ukraine (Ukraine); STFC (United Kingdom); NSF (USA). We also
 316 acknowledge the support received from the ERC under FP7 and the Region Auvergne.

References

- [1] M. Kobayashi and T. Maskawa, *CP-violation in the renormalizable theory of weak interaction*, Progress of Theoretical Physics **49** (1973) 652.
- [2] LHCb collaboration, R. Aaij *et al.*, *Measurement of the $B_s^0 - \bar{B}_s^0$ oscillation frequency Δm_s in $B_s^0 \rightarrow D_s(3)\pi$ decays*, Phys. Lett. **B709** (2011) 177, [arXiv:1112.4311](#).
- [3] CDF collaboration, A. Abulencia *et al.*, *Observation of $B_s^0 - \bar{B}_s^0$ oscillations*, Phys. Rev. Lett. **97** (2006) 242003.
- [4] A. Bazavov *et al.*, *Neutral B-meson mixing from three-flavor lattice QCD: determination of the $SU(3)$ -breaking ratio ξ* , [arXiv:1205.7013](#).
- [5] Heavy Flavor Averaging Group, Y. Amhis *et al.*, *Averages of b-hadron, c-hadron, and τ -lepton properties as of early 2012*, [arXiv:1207.1158](#).
- [6] BaBar collaboration, P. del Amo Sanchez *et al.*, *Study of $B \rightarrow X\gamma$ decays and determination of $|V_{td}/V_{ts}|$* , Phys. Rev. **D82** (2010) 051101, [arXiv:1005.4087](#).
- [7] Belle collaboration, K. Abe *et al.*, *Observation of $b \rightarrow d\gamma$ and determination of $|V_{td}/V_{ts}|$* , Phys. Rev. Lett. **96** (2006) 221601, [arXiv:hep-ex/0506079](#).
- [8] BaBar collaboration, B. Aubert *et al.*, *Branching fraction measurements of $B^+ \rightarrow \rho^+\gamma$, $B^0 \rightarrow \rho^0\gamma$, and $B^0 \rightarrow \omega\gamma$* , Phys. Rev. Lett. **98** (2007) 151802, [arXiv:hep-ex/0612017](#).
- [9] T. Hurth and M. Nakao, *Radiative and electroweak penguin decays of B mesons*, Ann. Rev. Nucl. Part. Sci. **60** (2010) 645, [arXiv:1005.1224](#).
- [10] A. Buras *et al.*, *Universal unitarity triangle and physics beyond the standard model*, Phys. Lett. **B500** (2001) 161, [arXiv:hep-ph/0007085](#).
- [11] T. Feldmann and T. Mannel, *Minimal flavour violation and beyond*, JHEP **02** (2007) 067, [arXiv:hep-ph/0611095](#).
- [12] R. Barbieri, D. Buttazzo, F. Sala, and D. M. Straub, *Less minimal flavour violation*, [arXiv:1206.1327](#).
- [13] J. J. Wang, R. M. Wang, Y. G. Xu, and Y. D. Yang, *The rare decays $B^+ \rightarrow \pi^+\ell^+\ell^-$, $\rho^+\ell^+\ell^-$, $B^0 \rightarrow \mu^+\mu^-$ in the R-parity violating supersymmetry*, Phys. Rev. **D77** (2008) 014017, [arXiv:0711.0321](#).
- [14] Belle collaboration, J. Wei *et al.*, *Search for $B \rightarrow \pi\ell^+\ell^-$ decays at Belle*, Phys. Rev. **D78** (2008) 011101, [arXiv:0804.3656](#).
- [15] LHCb collaboration, R. Aaij *et al.*, *Differential branching fraction and angular analysis of the $B^+ \rightarrow K^+\mu^+\mu^-$ decay*, [arXiv:1209.4284](#).

- 350 [16] LHCb collaboration, A. A. Alves Jr. *et al.*, *The LHCb detector at the LHC*, JINST **3**
351 (2008) S08005.
- 352 [17] V. V. Gligorov, C. Thomas, and M. Williams, *The HLT inclusive B triggers*, LHCb-
353 PUB-2011-016.
- 354 [18] R. Aaij and J. Albrecht, *Muon triggers in the high level trigger of LHCb*, LHCb-
355 PUB-2011-017.
- 356 [19] T. Sjöstrand, S. Mrenna, and P. Skands, *PYTHIA 6.4 Physics and manual*, JHEP **05**
357 (2006) 026, arXiv:hep-ph/0603175.
- 358 [20] I. Belyaev *et al.*, *Handling of the generation of primary events in GAUSS, the LHCb*
359 *simulation framework*, Nuclear Science Symposium Conference Record (NSS/MIC)
360 **IEEE** (2010) 1155.
- 361 [21] D. J. Lange, *The EvtGen particle decay simulation package*, Nucl. Instrum. Meth.
362 **A462** (2001) 152.
- 363 [22] P. Golonka and Z. Was, *PHOTOS Monte Carlo: a precision tool for QED corrections*
364 *in Z and W decays*, Eur. Phys. J. **C45** (2006) 97, arXiv:hep-ph/0506026.
- 365 [23] GEANT4 collaboration, J. Allison *et al.*, *Geant4 developments and applications*,
366 IEEE Trans. Nucl. Sci. **53** (2006) 270; GEANT4 collaboration, S. Agostinelli *et al.*,
367 *GEANT4: A simulation toolkit*, Nucl. Instrum. Meth. **A506** (2003) 250.
- 368 [24] M. Clemencic *et al.*, *The LHCb simulation application, GAUSS: design, evolution and*
369 *experience*, J. of Phys.: Conf. Ser. **331** (2011) 032023.
- 370 [25] Particle Data Group, J. Beringer *et al.*, *Review of particle physics*, Phys. Rev. **D86**
371 (2012) 010001.
- 372 [26] L. Breiman, J. H. Friedman, R. A. Olshen, and C. J. Stone, *Classification and*
373 *regression trees*, Wadsworth international group, Belmont, California, USA, 1984.
- 374 [27] Y. Freund and R. E. Schapire, *A decision-theoretic generalization of on-line learning*
375 *and an application to boosting*, Jour. Comp. and Syst. Sc. **55** (1997) 119.
- 376 [28] T. Skwarnicki, *A study of the radiative cascade transitions between the Upsilon-prime*
377 *and Upsilon resonances*, Ph.D. thesis, Institute of Nuclear Physics, Krakow, 1986,
378 DESY-F31-86-02.
- 379 [29] A. Ali, P. Ball, L. T. Handoko, and G. Hiller, *Comparative study of the decays*
380 *$B \rightarrow (K, K^*)\ell^+\ell^-$ in standard model and supersymmetric theories*, Phys. Rev. **D61**
381 (2000) 074024, arXiv:hep-ph/9910221.

- 382 [30] A. Ali, E. Lunghi, C. Greub, and G. Hiller, *Improved model independent analy-*
383 *sis of semileptonic and radiative rare B decays*, Phys. Rev. **D66** (2002) 034002,
384 [arXiv:hep-ph/0112300](#).
- 385 [31] H. Asatryan, H. Asatrian, C. Greub, and M. Walker, *Two loop virtual correc-*
386 *tions to $B \rightarrow X_s \ell^+ \ell^-$ in the standard model*, Phys. Lett. **B507** (2001) 162,
387 [arXiv:hep-ph/0103087](#).
- 388 [32] C. Bobeth, M. Misiak, and J. Urban, *Photonic penguins at two loops and $m(t)$ depen-*
389 *dence of $BR[B \rightarrow X_s \ell^+ \ell^-]$* , Nucl. Phys. **B574** (2000) 291, [arXiv:hep-ph/9910220](#).
- 390 [33] P. Ball and R. Zwicky, *New results on $B \rightarrow \pi, K, \eta$ decay form factors from light-cone*
391 *sum rules*, Phys. Rev. **D71** (2005) 014015, [arXiv:hep-ph/0406232](#).